NASA TECHNICAL NOTE

NASA TN D-2628

C.1

NASA TN D-2628

WIND-TUNNEL INVESTIGATION OF A LIFTING ROTOR OPERATING AT TIP-SPEED RATIOS FROM 0.65 TO 1.45

by Julian L. Jenkins, Jr.

Langley Research Center
Langley Station, Hampton, Va.

NATIONAL AERONAUTICS AND SPACE ADMINISTRATION • WASHINGTON, D. C. • FEBRUARY 1965

WIND-TUNNEL INVESTIGATION OF A LIFTING ROTOR OPERATING AT TIP-SPEED RATIOS FROM 0.65 TO 1.45

By Julian L. Jenkins, Jr.

Langley Research Center
Langley Station, Hampton, Va.

NATIONAL AERONAUTICS AND SPACE ADMINISTRATION

For sale by the Office of Technical Services, Department of Commerce,
Washington, D.C. 20230 -- Price $1.00

WIND-TUNNEL INVESTIGATION OF A LIFTING ROTOR OPERATING AT TIP-SPEED RATIOS FROM 0.65 TO 1.45

By Julian L. Jenkins, Jr.
Langley Research Center

SUMMARY

A wind-tunnel investigation of a 15-foot-diameter rotor was made to explore rotor operation at tip-speed ratios near 1.00. A two-blade teetering-type rotor system was tested in the Langley full-scale tunnel for tip-speed ratios from 0.65 to 1.45. Representative data were compared with theoretical calculations to indicate the predictability of the experimental trends obtained.

The results indicate that rotor efficiencies as high as 13 can be attained at the highest tip-speed ratio investigated. Although high rotor efficiencies are thus shown to be possible, a problem requiring further study was noted. The slope of the variation of rotor thrust with collective pitch was negative for a constant disk attitude at tip-speed ratios greater than 1.00. The negative slope resulted primarily from the increased sensitivity of the rotor longitudinal flapping response with respect to collective pitch compared with the sensitivity of the flapping response with respect to angle of attack. The theoretical calculations of the rotor characteristics also indicated this reversal phenomenon.

INTRODUCTION

The high-speed capability of rotary-wing aircraft has been the subject of much experimental and theoretical study in recent years. These studies indicate that a compounding of components (auxiliary propulsion system or lift augmentation or both) will be required as speeds surpass 200 knots. Also, rotor speeds must be reduced to avoid the sharp power rise which accompanies compressibility effects. (See, for example, ref. 1.) Consequently, the operating tip-speed ratio of a compound configuration will be much higher than that of a pure helicopter. These higher tip-speed-ratio requirements have stimulated interest in rotor operation at tip-speed ratios greater than 1.00. In addition, theoretical studies have indicated improvements in rotor efficiency (i.e., higher rotor lift-drag ratios) at these high tip-speed ratios.

The present wind-tunnel investigation of a 15-foot-diameter rotor was undertaken to explore the lifting capability at tip-speed ratios from about 0.65 to 1.45. The tests were conducted in the Langley full-scale tunnel on a two-blade teetering-type rotor system. Measurements of rotor forces, torque, and flapping motions were recorded at rotor tip-path-plane angles of attack of 0.5° and 5.5° for the tip-speed ratios. Representative data are compared with theoretical calculations to indicate the predictability of the experimental trends obtained. A photograph of tufts attached to the blade surface is presented to illustrate the flow over the rotor blades.

SYMBOLS

The positive directions of forces and angles are shown in figure 1.

A_o blade collective pitch angle, deg

a blade-section lift-curve slope, 5.55 per radian

a' angle between control axis and resultant-force vector in longitudinal plane, deg

a_1 first-harmonic longitudinal flapping angle, deg

b number of blades

b_1 first-harmonic lateral flapping angle, deg

C_H rotor drag coefficient, $\dfrac{H}{\rho\pi R^2(\Omega R)^2}$

C_Q rotor torque coefficient, $\dfrac{Q}{\rho\pi R^2(\Omega R)^2 R}$

C_R rotor resultant-force coefficient, $\left(C_T{}^2 + C_H{}^2\right)^{1/2}$

C_T rotor thrust coefficient, $\dfrac{T}{\rho\pi R^2(\Omega R)^2}$

c blade chord, ft

H longitudinal component of rotor resultant force perpendicular to shaft axis, lb

I_h mass moment of inertia of blade about flapping hinge, slug-ft^2

$(L/D)_r$ equivalent rotor lift-drag ratio, ratio of rotor lift to sum of rotor profile and induced powers expressed as an equivalent drag

Q rotor torque, ft-lb

R	blade radius measured from center of rotation, ft
T	rotor thrust, lb
V	velocity, ft/sec
α	rotor control-axis angle of attack, deg
α_r	blade-element angle of attack, deg
α_s	rotor shaft angle of attack, deg
α_{TPP}	rotor tip-path-plane angle of attack, deg
γ	mass constant of rotor blade (blade Lock number), $\frac{\rho acR^4}{I_h}$
μ	rotor tip-speed ratio, $\frac{V}{\Omega R}$
ρ	mass density of air, slugs/cu ft
σ	rotor solidity, $bc/\pi R$
ψ	blade azimuth angle measured from downwind position of rotor in direction of rotation, deg
Ω	rotor angular velocity, rad/sec

APPARATUS

The test apparatus and photographic equipment as installed in the Langley full-scale tunnel are shown in figure 2. A large ground-reflection plane was installed below the rotor to minimize the jet-boundary corrections.

Rotor

The rotor was a two-blade teetering type with no built-in coning angle. The rotor had a diameter of 15.25 feet, a constant blade chord of 1.16 feet, and a corresponding solidity σ of 0.097. The blades were untwisted NACA 0012 airfoil sections and had a Lock number γ of 5.05. Carborundum grains (0.012-inch mean grain diameter) were sparsely distributed on a 0.25-inch strip along the blade span on the upper surface at the 10-percent-chord station. The purpose of this roughness was to avoid variations in section characteristics by fixing the transition point. Two tufts were attached at each of six spanwise stations. The blade stiffness both in bending and in torsion was large in relation to the rotor loads; therefore, periodic twist caused by air loads is believed to have been small.

Instrumentation

Rotor thrust and torque were measured by strain-gage instrumentation located within the rotor-support tower (fig. 3). Thrust was corrected for loads carried by the blade-pitch-change rods, and the friction torque of the swash plate was subtracted from the rotor-torque measurements. The total drag of the model was measured with the tunnel drag balance. Rotor longitudinal force was obtained by subtracting the tares obtained with the blades removed from the rotor-operating data. Blade flapping motions were sensed by strain gages and recorded on an oscillograph. A Fourier analysis was performed on these data to determine the first-harmonic flapping coefficients. Rotor rotational speed was sensed by a magnetic pickup and recorded on an oscillograph.

The overall accuracies of the data are believed to be within the following limits:

C_T	±0.00080
C_H	±0.00055
C_Q	±0.000075
Rotor tip speed, fps	±1
Rotor tip-speed ratio	±0.01
Shaft angle of attack, collective pitch, lateral cyclic pitch, and flapping motions, deg	±0.25
Longitudinal cyclic pitch, deg	±0.50

Tuft Photographs

Multiexposure photographs of the tufts attached to the rotor blades were made with the camera and flash equipment shown in figure 2. Five exposures, spaced at intervals of about 40° in azimuth on the retreating side of the rotor disk, were made during one rotor revolution. An additional five exposures, at intermediate azimuth positions, were made about 1 minute after the first photographs.

TESTS AND CORRECTIONS

All tests were run at a rotor tip speed (ΩR) of about 110 feet per second, which corresponds to a hovering-tip Reynolds number of about 0.81×10^6. Performance measurements were made at shaft angles of attack α_s of 0.5° and 5.5° with the tip-path plane trimmed normal to the shaft for all thrust settings; therefore, the tip-path-plane angles of attack α_{TPP} were also 0.5° and 5.5°. No jet-boundary corrections were applied; with the tunnel configurations used, they should be negligible for the present range of test conditions. (See ref. 2.)

RESULTS AND DISCUSSION

Measured Rotor Characteristics

The experimental data obtained from wind-tunnel tests of a teetering-type rotor operating at tip-speed ratios from 0.65 to 1.45 are presented in figure 4. These data are presented for shaft angles of attack of 0.5° and 5.5° with the tip-path plane of the rotor trimmed normal to the shaft. This presentation highlights a trend in the rotor-thrust variation which is not believed to have been previously reported; that is, the slope of the variation of rotor thrust with collective pitch becomes increasingly negative with increasing tip-speed ratio for tip-speed ratios greater than 1.00. As shown in reference 3, for the same rotor, the variation of thrust with collective pitch has a positive slope for tip-speed ratios to 0.54 for the tip-path-plane angles from -9.5° to 10.5°. This same positive slope is evident in the present test for tip-speed ratios below 0.94.

The trends shown by these results suggest that at a tip-speed ratio of approximately 1.00 the variation of thrust with collective pitch is zero for a constant rotor-disk attitude. In other words, increasing collective pitch and retrimming the rotor tip-path plane to its original attitude with cyclic control produces no change in rotor thrust at a tip-speed ratio of 1.00. At higher tip-speed ratios, this same procedure produces a loss in thrust and is, in effect, a control reversal in the sense that the combination of collective and cyclic pitch inputs which produces a positive thrust increment at conventional tip-speed ratios now produces a negative thrust increment.

This reversal could be quite disconcerting to a pilot of a compound helicopter with manual control of the rotor because a reduction in collective pitch and longitudinal cyclic control is required in order to increase rotor thrust and simultaneously to maintain a relatively constant rotor attitude. Constant rotor attitude is desired at high tip-speed ratios in order to maintain a safe rotor-fuselage clearance during maneuvers or gusts. If the rotor is controlled automatically rather than manually, specific consideration of the problem of rotor thrust reversal will be required during the design stage to ensure acceptable operation over the entire speed range.

Rotor Lifting Efficiency

Theoretical studies have indicated that very high rotor efficiencies (ratio of rotor lift to equivalent drag $(L/D)_r$) are possible at high tip-speed ratios. The experimental lift-drag ratios obtained for this rotor are presented in figure 5. These curves were obtained from faired curves of rotor thrust, torque, and drag, and thus eliminated the scatter in the data that occurs when dealing with ratios of relatively small forces. It is important to note that these values are conservative because the tests were made with tufts on the blades. In general, the lift-drag ratios are much higher than those indicated in reference 3 for this same rotor operating at lower tip-speed ratios; and for tip-speed ratios of 1.25 and 1.45, there is an indication of even greater lift-drag ratios with further reductions in collective pitch. These high values are not the total lift-drag ratio of the aircraft, but they do indicate that the penalty for operating the rotor at high speeds can be reduced.

Rotor Stability Derivatives

In order to gain insight into the factors that influence the thrust reversal shown by these tests, an investigation of the rotor stability derivatives is required. The derivative of thrust coefficient with respect to collective pitch $\Delta C_T/\Delta A_o$ is determined for a constant disk attitude $\left(\alpha_{TPP} = \text{Constant}\right)$. The resulting equation is

$$\left(\frac{\Delta C_T}{\Delta A_o}\right)_{\Delta\alpha_{TPP}=0} = \frac{\partial C_T}{\partial A_o} - \frac{\partial C_T}{\partial \alpha}\frac{\partial a_1/\partial A_o}{1 + \frac{\partial a_1}{\partial \alpha}} \tag{1}$$

It can be seen that when $\Delta C_T/\Delta A_o$ has a positive value, a collective pitch increase results in a positive thrust increment, but when $\Delta C_T/\Delta A_o$ is negative, a collective pitch increase results in a negative thrust increment.

The relative magnitudes of the four derivatives in equation (1) and their variation with tip-speed ratio can be seen in figure 6. The derivatives with respect to collective pitch at constant angle of attack and the derivatives with respect to angle of attack at constant collective pitch were obtained from cross plots of the thrust and longitudinal flapping data. For the data presented in figure 6, the derivative $\Delta C_T/\Delta A_o$, determined by the equation, becomes zero at a tip-speed ratio of approximately 1.00. Below $\mu = 1.00$ the derivative $\Delta C_T/\Delta A_o$ is positive, and above $\mu = 1.00$ the derivative is negative. Since the trend exhibited here is the same as that shown in figure 4, equation (1) can be utilized to examine the contribution of the individual stability derivatives to the total thrust derivative $\Delta C_T/\Delta A_o$.

Both of the thrust derivatives increase rapidly with increasing tip-speed ratio; however, the derivative of thrust with respect to collective pitch increases slightly faster than the derivative of thrust with respect to angle of attack. It can be seen from equation (1) that this trend delays the point at which the equation goes to zero and thus delays the reversal in slope of the rotor thrust shown in figure 4. The relative magnitudes of the flapping derivatives reveal the cause of the thrust reversal exhibited by this rotor. With an increase in tip-speed ratio, the rapid increase in the flapping derivative with respect to collective pitch causes the term $\dfrac{\partial a_1/\partial A_o}{1 + \frac{\partial a_1}{\partial \alpha}}$ in equation (1) to become greater than 1.0; therefore, $\Delta C_T/\Delta A_o$ approaches zero and then becomes negative.

Comparison of Measured and Calculated Rotor Characteristics

The measured thrust and longitudinal flapping coefficients from two of the test runs are compared with theoretical calculations to indicate the predictability of the thrust reversal trends exhibited by this rotor. The comparisons are made for only these parameters because these tests were made with tufts on the blades and thus a comparison of torque and in-plane forces would be invalid. The calculations were carried out on a high-speed, electronic data-processing machine, which was programed according to the equations presented in reference 4. These equations account for stall, tip losses, blade cutout, and the reversed velocity. The results are presented in figure 7 for tip-speed ratios of 0.94 and 1.45. It is important to note that the trends of the thrust curves including the slope reversal are well defined, although the magnitudes of the calculated thrusts are high. The longitudinal flapping is also overestimated in both cases, and for a tip-speed ratio of 1.45 the slope of the curve is not as well defined as that for a tip-speed ratio of 0.94.

These discrepancies between measured and calculated data can be explained in part by the relatively poor accuracy of the absolute values of the measured input quantities (A_o and α) and the overall sensitivity of the rotor thrust and flapping response to small variations in these quantities. For example, at a tip-speed ratio of 1.45, the thrust coefficient changes at the rate of 0.0051 per degree of angle of attack and 0.0063 per degree of collective pitch (fig. 6); consequently, small variations in the input values can produce very different computed results. In spite of the changes in absolute magnitudes of the computed thrust and flapping angle with small variations in the input quantities, sample calculations indicated that the thrust reversal trend was unaffected. Thus, the discrepancies between the measured and calculated values are apparently related to factors which do not greatly affect the reversal, and hence the theoretical analysis is considered to provide an adequate method for confirming and explaining the nature of the reversal phenomenon.

Theoretical Thrust Distribution

An indication of the areas on the rotor disk that affect the reversal phenomenon can be seen in figure 8, where the variation of calculated thrust with azimuth angle for two values of collective pitch at tip-speed ratios of 0.94 and 1.45 is presented. These curves correspond to the data presented in figure 7. At a tip-speed ratio of 0.94 (fig. 8(a)), the increases in thrust near $\psi = 20^\circ$ and $\psi = 160^\circ$ as the collective pitch is increased from 0° to 4° are essentially offset by the losses of thrust near $\psi = 90^\circ$ and $\psi = 270^\circ$ due to the longitudinal cyclic pitch required to retrim the rotor disk attitude. It is of interest to note that the loss of thrust near $\psi = 270^\circ$ for $A_o = 4^\circ$ results from a decrease in the effective blade-section angles of attack which is caused by the compounding of positive collective pitch, positive cyclic pitch, and the reversed velocity over the blade. Thus, when the collective pitch is increased and cyclic pitch is increased so as to keep a constant disk attitude, the net result for this tip-speed ratio is a relatively constant rotor thrust.

At the higher tip-speed ratio ($\mu = 1.45$) in figure 8(b), the effect of increasing collective pitch and retrimming rotor attitude is even more pronounced. In the region near $\psi = 270^\circ$, for 0° collective pitch a significant part of the total rotor thrust is produced. Increasing collective pitch by 4° and retrimming the rotor attitude results in an almost complete loss of thrust in the region from $\psi = 210^\circ$ to $\psi = 330^\circ$. The thrust remains relatively constant near $\psi = 20^\circ$ and $\psi = 160^\circ$ because of the extreme blade-section angles of attack in these regions. Thus there is a net loss in thrust for an increase of 4° in collective pitch when the rotor is retrimmed.

Correlation of Tuft Photographs with Theoretical

Blade-Section Angles of Attack

Calculated contours of lines of constant section angles of attack are presented in figure 9 to illustrate the severity of the blade-section angles of attack which exist for a tip-speed ratio of 1.45. These contours were calculated for a collective pitch of -0.66°, which corresponds to the actual measured value for the tuft photograph presented. It is apparent from the contours that increasing collective pitch will not produce further increases in thrust in the regions near $\psi = 20^\circ$ and $\psi = 180^\circ$ because the angles of attack are already greater than the approximate stall angle of 12°. This fact accounts for the relatively constant thrust in these regions shown in figure 8(b).

Interpretation of the tuft patterns is at best a difficult task because of the numerous factors which influence the tufts; however, where the ends of the tufts point toward the trailing edge of the blade in the reversed velocity region (i.e., section angles of attack greater than 90°), the predominant effect is believed to be local flow separation. At an angle of attack of 90° the flow is obviously separated, whereas at an angle of attack of 170° two-dimensional airfoil data indicate that the flow is reattached. For the condition presented, local flow separation is apparent for most of the trailing-edge tufts in the region near the contour line of 160°. The tufts indicate a reattachment of the flow in the region of the contour line of 170°. It is interesting to consider the possibility of increasing this region by operating at higher tip-speed ratios with very low values of collective pitch and a more positive rotor attitude.

CONCLUDING REMARKS

Results of a wind-tunnel investigation of a 15-foot-diameter rotor operating at tip-speed ratios from 0.65 to 1.45 indicate that rotor efficiencies as high as 13 can be attained at the highest tip-speed ratio. Although high rotor efficiencies are thus shown to be possible, a problem requiring further study was noted. The slope of the variation of rotor thrust with collective pitch was negative for a constant disk attitude at tip-speed ratios greater than 1.00. The negative slope resulted primarily from the increased sensitivity of the rotor longitudinal flapping response with respect to collective pitch compared with the sensitivity of the flapping response with respect to angle of attack. The theoretical calculations of the rotor characteristics also indicated this reversal phenomenon.

Langley Research Center,
National Aeronautics and Space Administration,
Langley Station, Hampton, Va., October 12, 1964.

REFERENCES

1. Fradenburgh, Evan A.: Aerodynamic Efficiency Potentials of Rotary Wing Aircraft. Proc. Sixteenth Ann. Natl. Forum, Am. Helicopter Soc., Inc., May 1960, pp. 20-30.

2. Heyson, Harry H.: Linearized Theory of Wind-Tunnel Jet-Boundary Corrections and Ground Effect for VTOL-STOL Aircraft. NASA TR R-124, 1962.

3. Sweet, George E.; Jenkins, Julian L., Jr.; and Winston, Matthew M.: Wind-Tunnel Measurements on a Lifting Rotor at High Thrust Coefficients and High Tip-Speed Ratios. NASA TN D-2462, 1964.

4. Gessow, Alfred; and Crim, Almer D.: A Method for Studying the Transient Blade-Flapping Behavior of Lifting Rotors at Extreme Operating Conditions. NACA TN 3366, 1955.

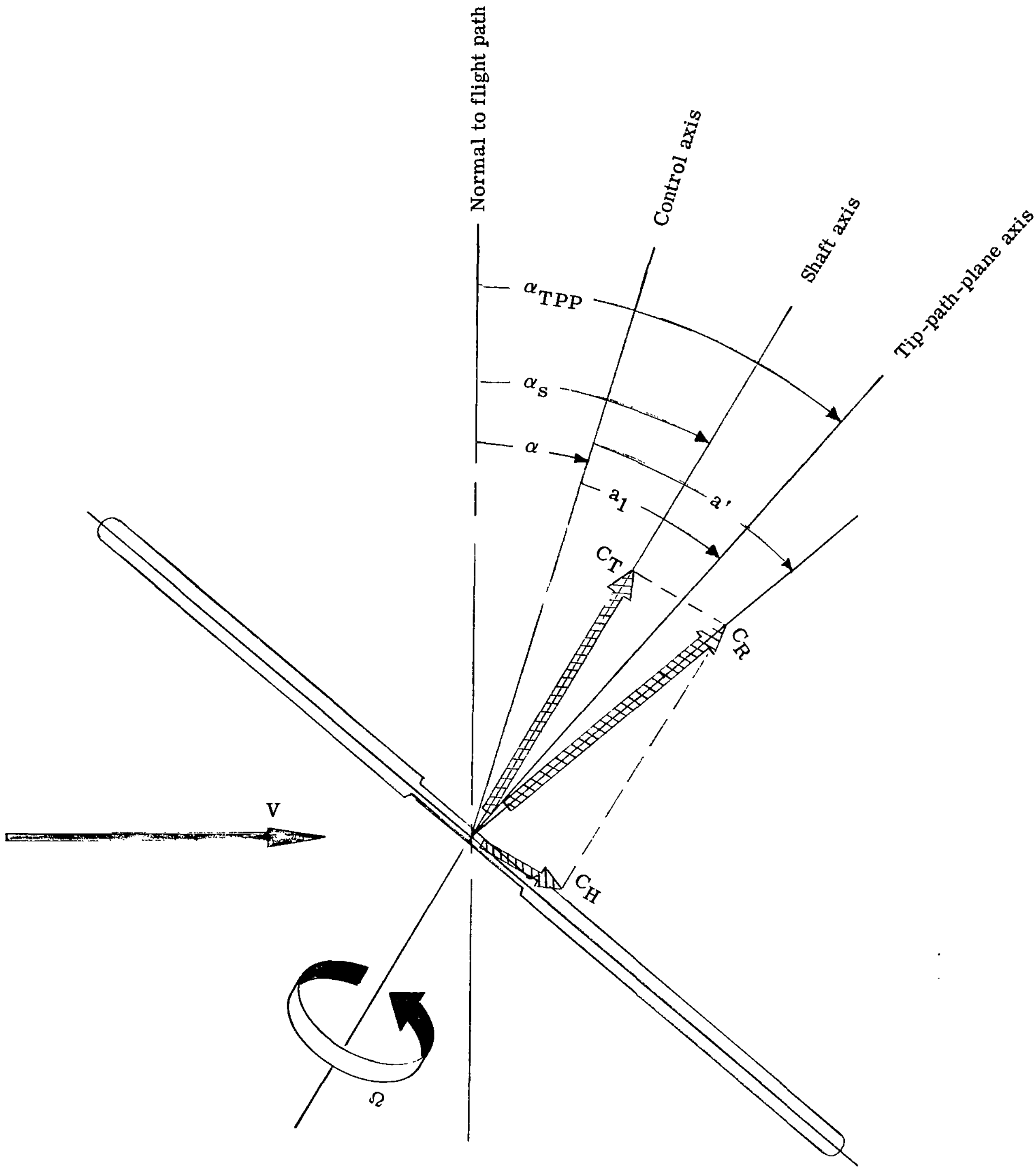

Figure 1.- Notation showing positive direction of forces and angles. Side view.

L-62-3093.1

Figure 2.- General view of test apparatus installed in Langley full-scale tunnel.

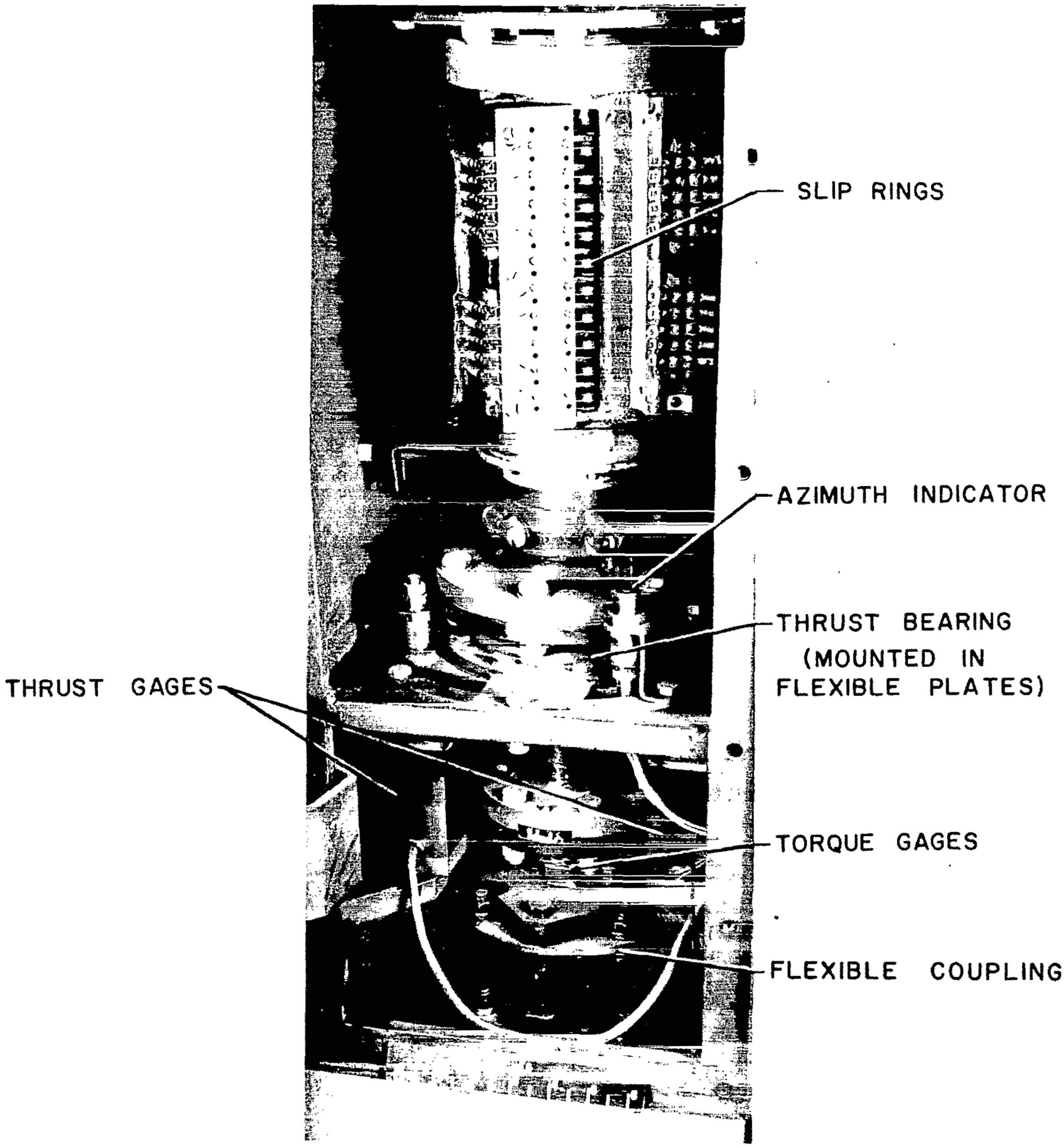

Figure 3.- Force measuring system. L-58-621a.1

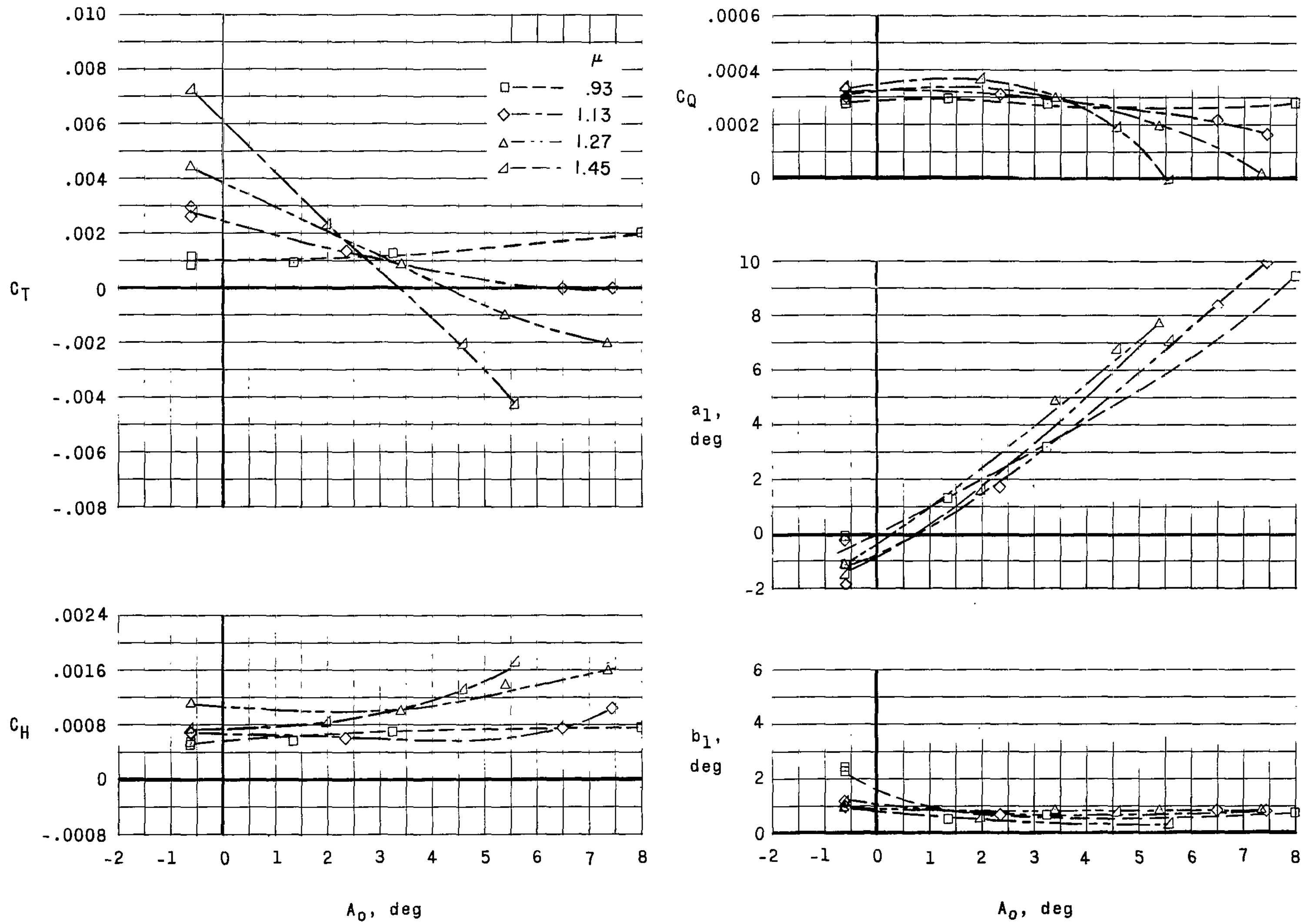

(a) $\alpha_{TPP} = 0.5^{\circ}$.

Figure 4.- Summary of rotor characteristics at constant disk attitudes.

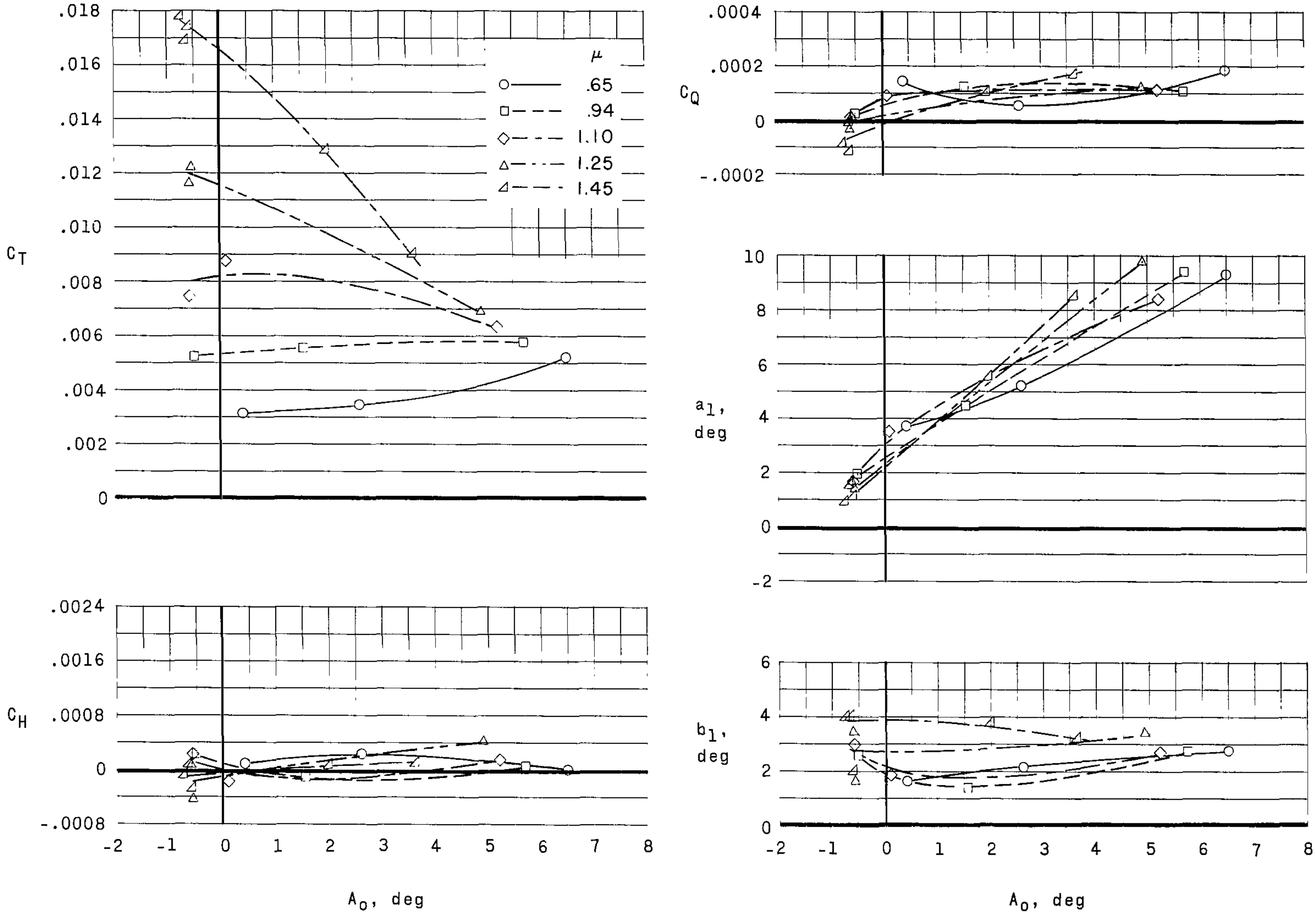

(b) $\alpha_{TPP} = 5.5^{\circ}$.

Figure 4.- Concluded.

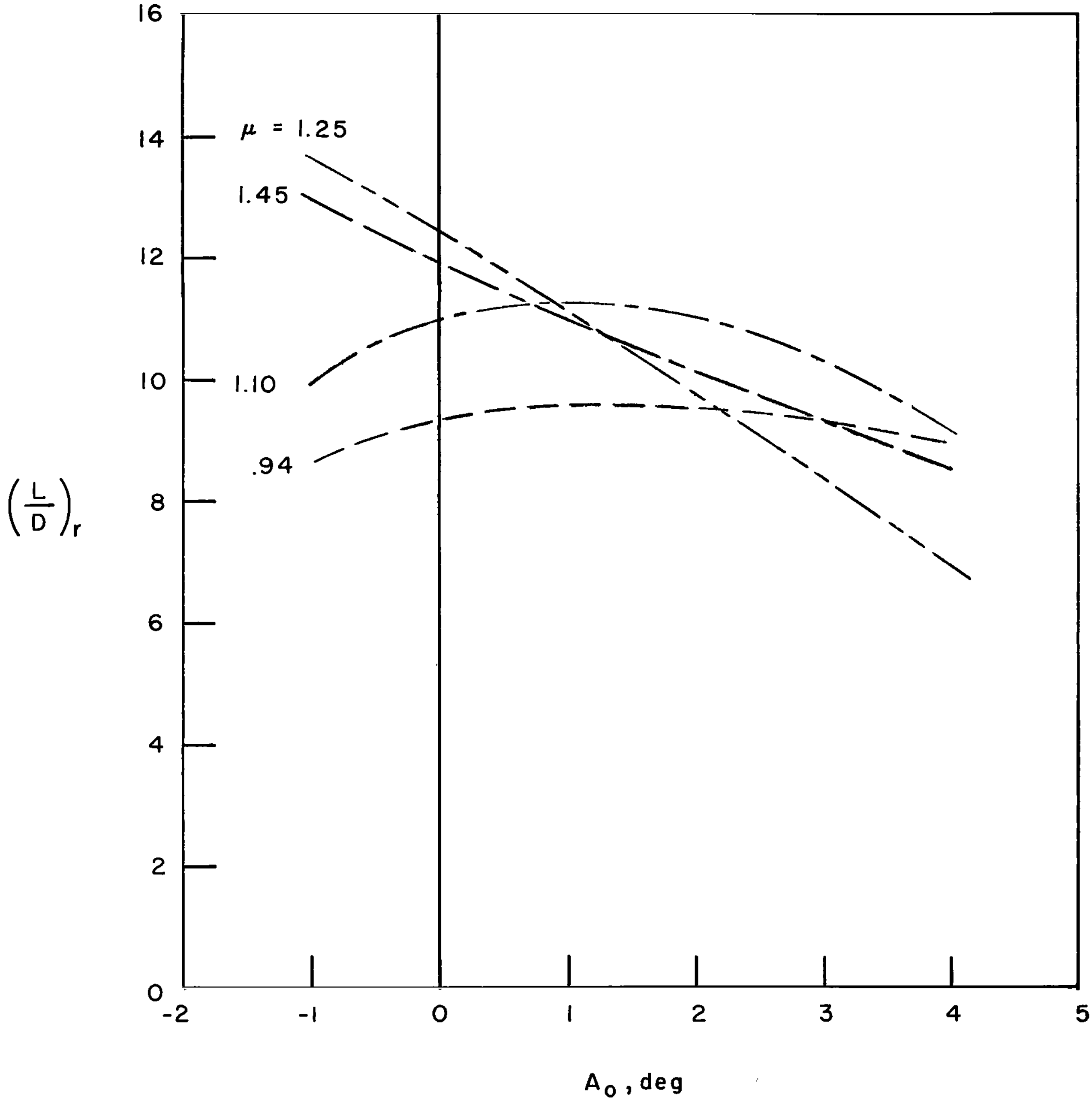

Figure 5.- Variation of equivalent rotor lift-drag ratio with collective pitch and tip-speed ratio. $\alpha_s = 5.5^{\circ}$.

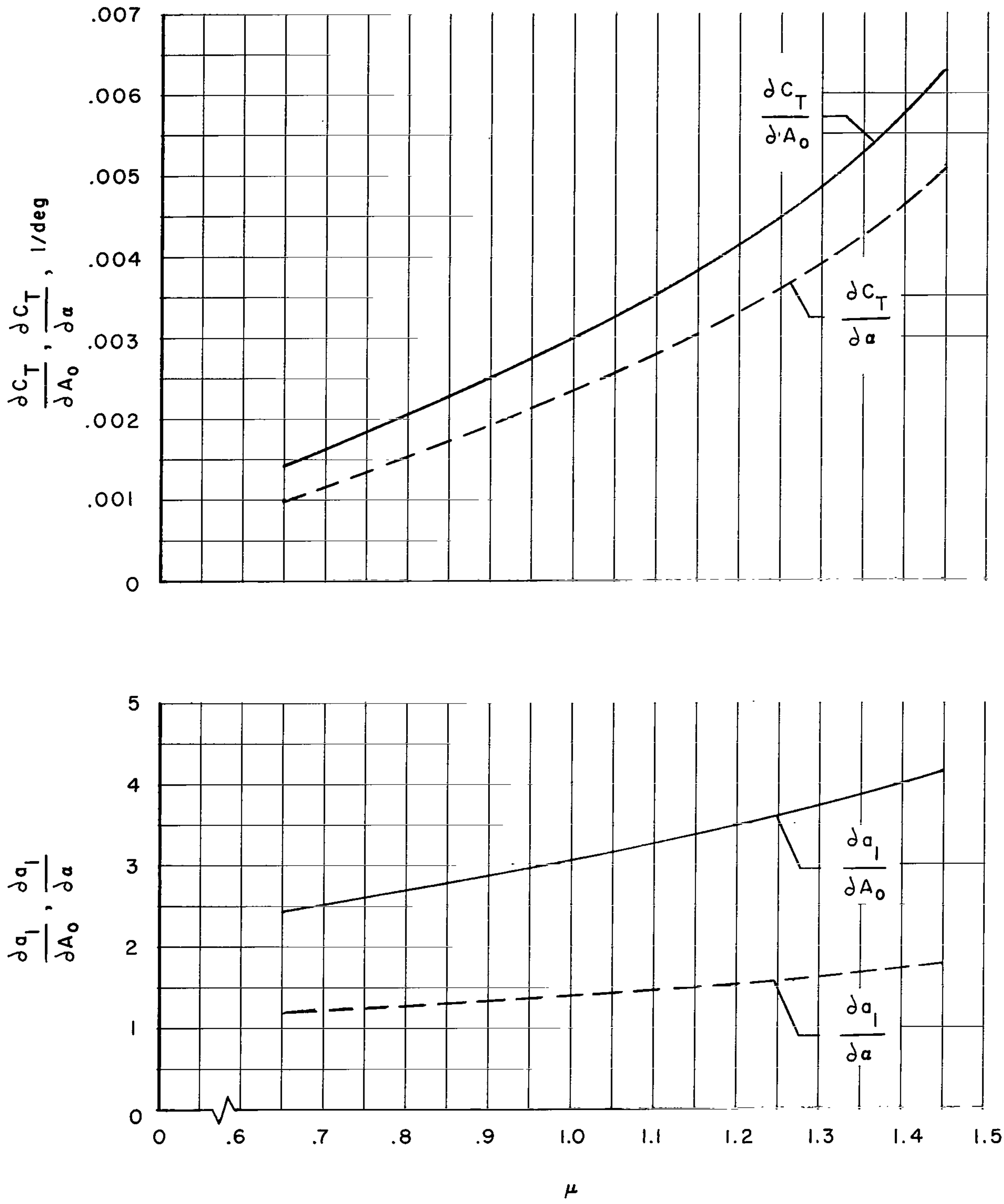

Figure 6.- Variation of rotor thrust and longitudinal flapping derivatives with tip-speed ratio.

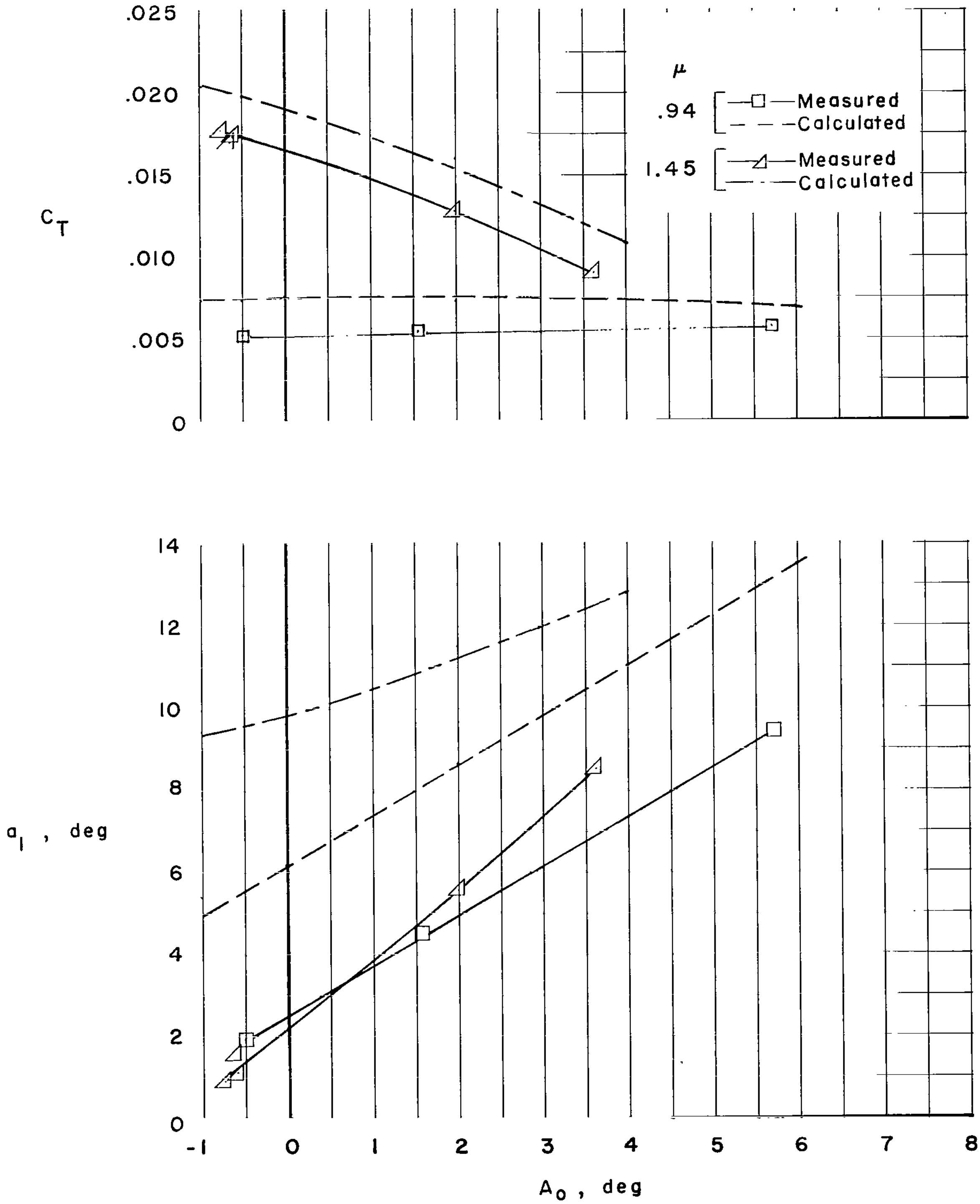

Figure 7.- Comparison of measured and calculated rotor thrust and longitudinal flapping. $\alpha_s = 5.5^{\circ}$.

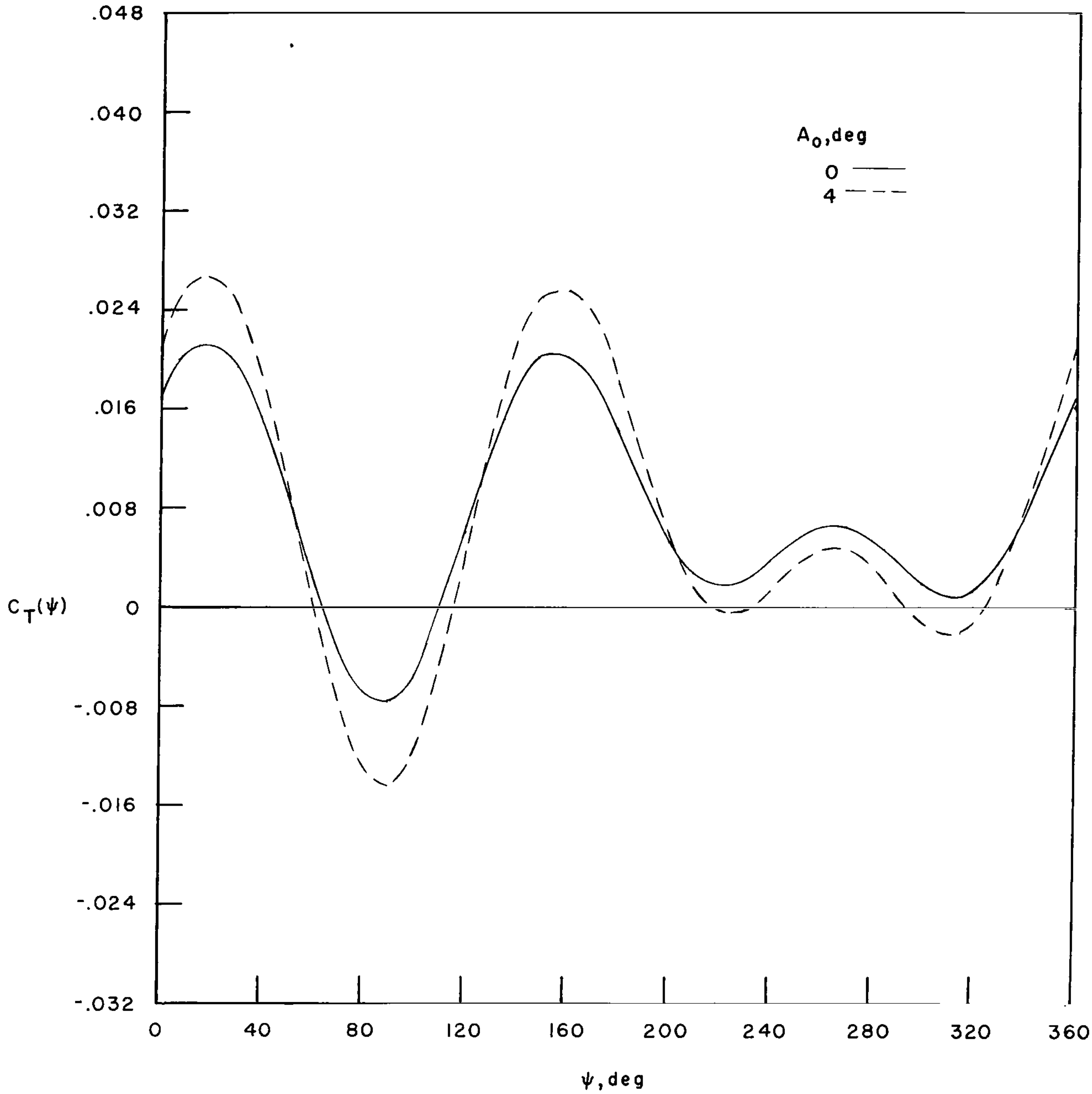

(a) $\mu = 0.94$.

Figure 8.- Variation of azimuth angle with calculated rotor thrust. $\alpha_s = 5.5^{\circ}$.

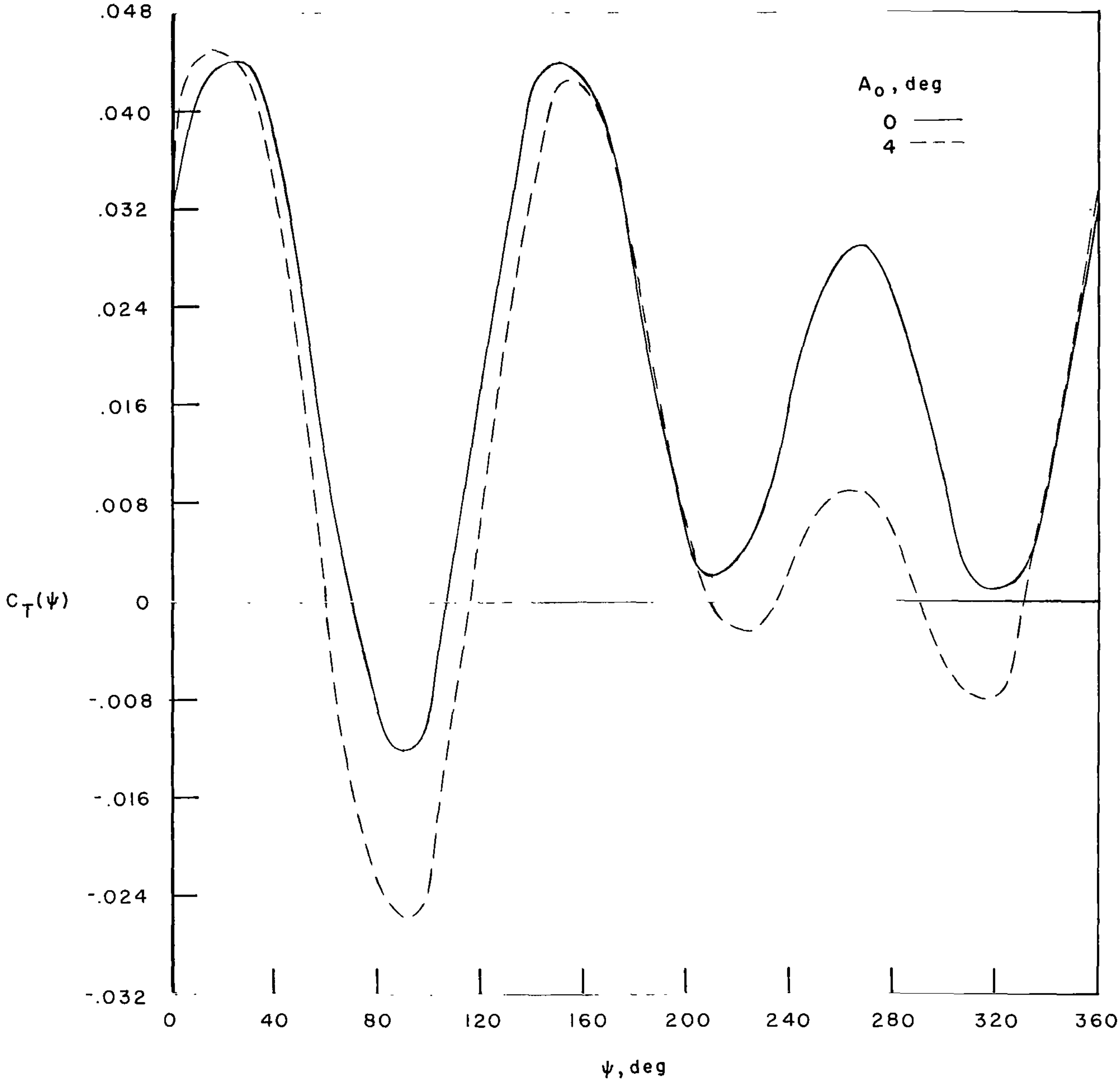

(b) $\mu = 1.45$.

Figure 8.- Concluded.

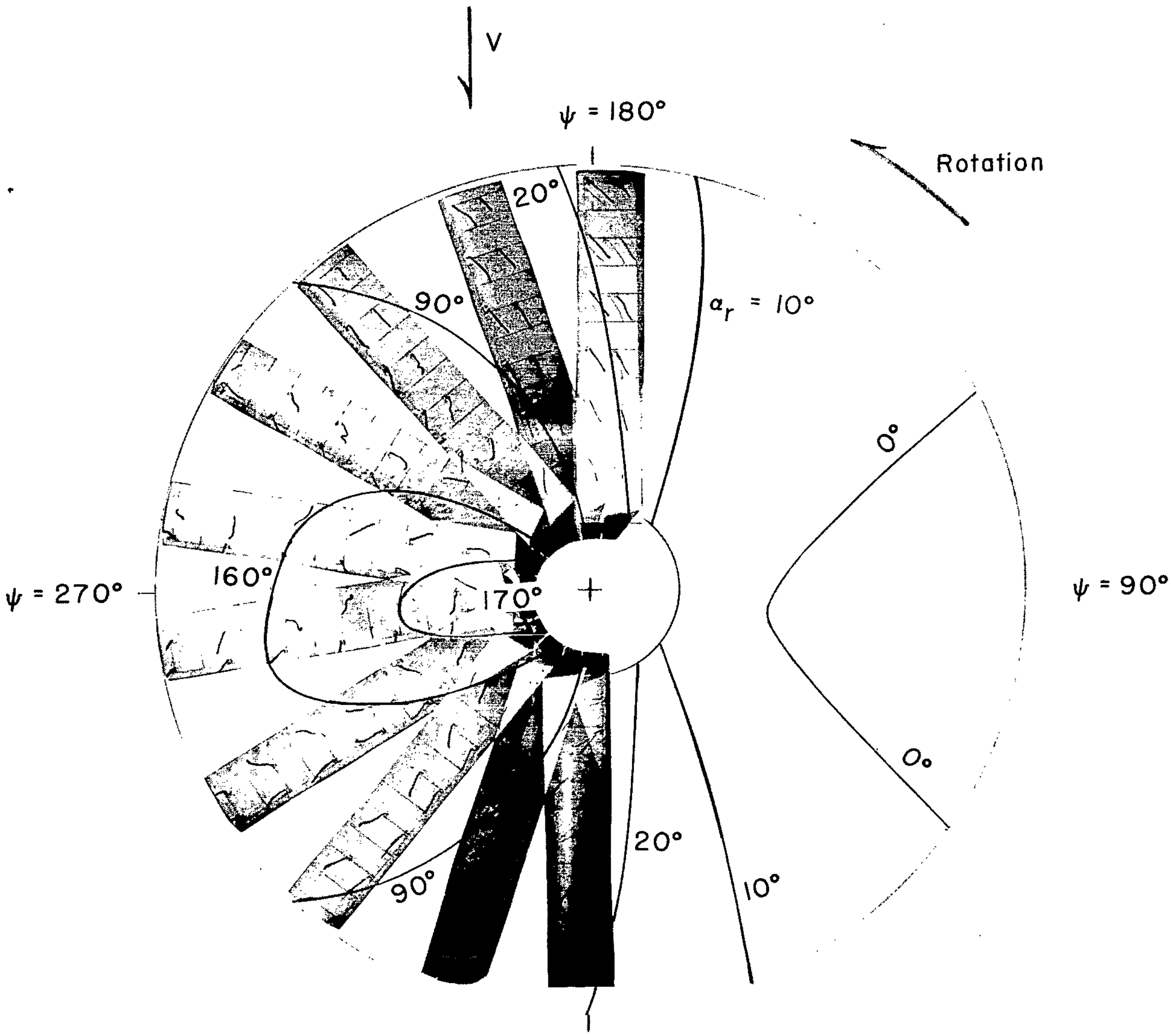

L-64-8380

Figure 9.- Comparison of tuft photograph with calculated contours of constant-section angle of attack for a tip-path-plane attitude of 5.5° and tip-speed ratio of 1.45.

NASA-Langley, 1965 L-4233

"The aeronautical and space activities of the United States shall be conducted so as to contribute . . . to the expansion of human knowledge of phenomena in the atmosphere and space. The Administration shall provide for the widest practicable and appropriate dissemination of information concerning its activities and the results thereof."

—NATIONAL AERONAUTICS AND SPACE ACT OF 1958

NASA SCIENTIFIC AND TECHNICAL PUBLICATIONS

TECHNICAL REPORTS: Scientific and technical information considered important, complete, and a lasting contribution to existing knowledge.

TECHNICAL NOTES: Information less broad in scope but nevertheless of importance as a contribution to existing knowledge.

TECHNICAL MEMORANDUMS: Information receiving limited distribution because of preliminary data, security classification, or other reasons.

CONTRACTOR REPORTS: Technical information generated in connection with a NASA contract or grant and released under NASA auspices.

TECHNICAL TRANSLATIONS: Information published in a foreign language considered to merit NASA distribution in English.

TECHNICAL REPRINTS: Information derived from NASA activities and initially published in the form of journal articles.

SPECIAL PUBLICATIONS: Information derived from or of value to NASA activities but not necessarily reporting the results of individual NASA-programmed scientific efforts. Publications include conference proceedings, monographs, data compilations, handbooks, sourcebooks, and special bibliographies.

Details on the availability of these publications may be obtained from:

SCIENTIFIC AND TECHNICAL INFORMATION DIVISION

NATIONAL AERONAUTICS AND SPACE ADMINISTRATION

Washington, D.C. 20546